River, Coastal and Estuarine Morphodynamics: RCEM2011

A parameter study on bank shear stresses in curved open channel flow by means of large-eddy simulation

Willem OTTEVANGER
Faculty of Civil Engineering and Geosciences, Delft University of Technology, the Netherlands

Koen BLANCKAERT
State Key Laboratory of Urban and Regional Ecology, Research Center for Eco-Environmental Sciences, Chinese Academy of Sciences, Beijing, China
Laboratory of Hydraulic Constructions (LCH). Ecole Polytechnique Fédérale de Lausanne (EPFL), Station 18, Lausanne, Switzerland
Faculty of Civil Engineering and Geosciences, Delft University of Technology, the Netherlands

Wim S.J. UIJTTEWAAL
Faculty of Civil Engineering and Geosciences, Delft University of Technology, the Netherlands

ABSTRACT: Meandering rivers and streams are a common planform in the world's populated areas. Furthermore the recent increased focus on renaturalization projects has lead policy makers to also consider the partial remeandering of previously trained rivers. Economic factors such as navigation, man-made infrastructure and valuable farm land set the boundary conditions for such rivers. Understanding the behavior of the near bank flow in schematized open channel bends could help in understanding the behavior of meandering rivers and predict locations of potential damage, as well as aid in the development of design criteria of stable river banks.

The interaction of the hydrodynamics with the bed and banks causes meandering river to change their course over time. Hickin and Nanson (1975) showed that the yearly migration rate in meandering rivers depends on the ratio of the river width to the radius of curvature B/R of a river bend. They showed that there is a peak migration rate at $(B/R)_{max}$ between 0.5 and 0.33. For milder curvature $B/R < (B/R)_{max}$, but also for sharper curvature $B/R > (B/R)_{max}$ the yearly migration rate is lower. The explanation for this behavior is lacking.

Curved open channel flows exhibit complex flow structures (such as the outer bank cell) near the outer bank. To model these flow structures requires flow solvers with advanced turbulence modeling capabilities. Large-eddy simulation is able to capture the complex flow structures occurring in curved open channel flows.

Using a well-validated large-eddy simulation code, a large set of axi-symmetric simulations (infinite length bend) were performed. The simulations are based on a wide range of mildly and sharply curved bends (represented by the parameter space B/R and $C_f^{-1}H/B$).

The results indicate that for $B/R > 0.1$ the magnitude of the bank shear stress decreases with increasing inverse aspect ratio H/B. The magnitude of the bank shear stress was found to increase strongly for small increasing B/R. For large increasing B/R the magnitude of the bank shear stress no longer increases, but even slightly decreases. The bed shear stress magnitude, however, still increases for large increasing B/R, which suggests that sharply curved channels tend to deepen rather than migrate laterally.

Furthermore, considering the bank shear stress to depend quadratically on the sum of the velocity excess and the bulk velocity multiplied by a bank friction factor $C_{f,bank}$, a correction factor $\psi_{outer\ bank}$ is derived. The correction factor $\psi_{outer\ bank}$, which depends on B/R and H/B, represents the increase of bank

friction factor compared to a straight channel flow due to the complex curved outer bank hydrodynamics.

1 INTRODUCTION

Meandering rivers are known to change their path over the course of time. Their lateral migration through the alluvial plain has intrigued many generations of scientists. Recently the recognition of the necessity of no longer neglecting ecological processes in the building of hydraulic constructions, has sparked the interest in including ecology into the standard demands of hydraulic constructions (e.g. remeandering of previously cutoff bends and eco-friendly banks).

The flow in river bends is three dimensional and can be described in detail by the three dimensional velocity vector given by the components v_i with the subscript i, which is either 's' for the streamwise, 'n' for the transverse or 'z' for the vertical direction (cf. Figure 1). The flow in streamwise direction is also referred to as primary flow, whereas the flow normal to the streamwise flow is referred to as secondary flow. The three dimensional flow in river bends consists of primary and secondary flow.

At the centre of the channel secondary flow a helical motion exists which shall be referred to as the 'centre region cell' (cf. Figure 1). Boussinesq (1868) and Thompson (1876) pioneered the investigation into the centre-region cell. The centre region cell is ascribed to the interaction of centrifugal forcing and the transverse hydrodynamic pressure gradient. It is very important for redistributing streamwise momentum (Kalkwijk & de Vriend 1980) as well as the formation of the transverse slope in a river (van Bendegom 1947, Olesen 1987). The centre-region cell is a well studied and important feature in curved river bends.

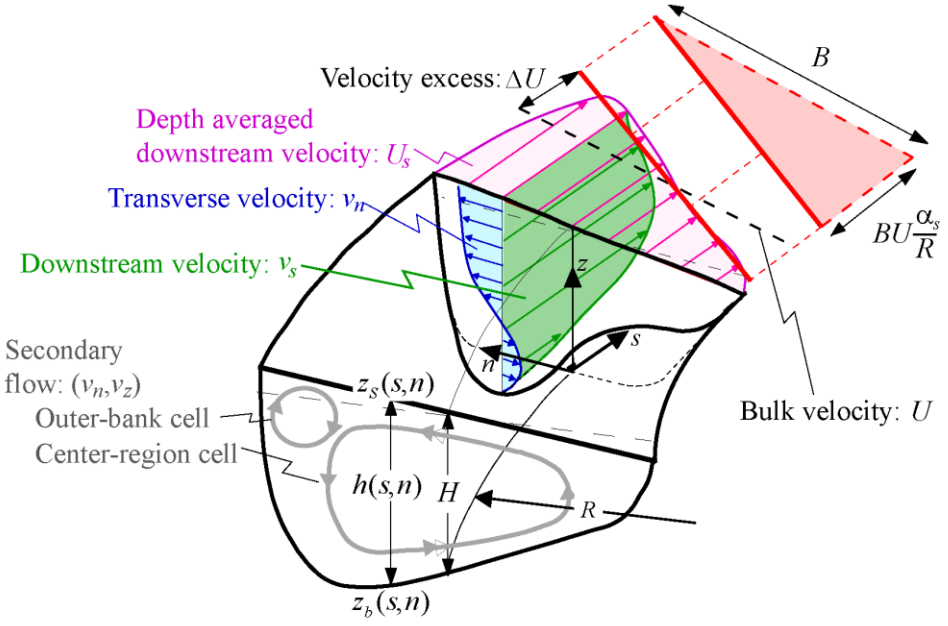

Figure 1 Bend geometry with definition of variables (modified from Blanckaert and de Vriend (2003)'s Figure 1)

Near the outer bank a smaller second secondary flow cell exists called the 'outer-bank cell'. In the context of natural river bends, Bathurst et al. (1977) first showed the outer bank cell in the River Severn. Bathurst et al. (1977) hypothesized the outer bank cell would endanger the outer bank stability as it would transfer high momentum fluid near the free surface to the outer bank. Blanckaert and Graf (2004) showed that the outer bank cell forms a buffer layer between the flow core and the bank thereby limiting the influence of the centre region cell, which is agreed to be an important factor for the outward transport of streamwise momentum.

Blanckaert & de Vriend (2004) and van Balen et al. (2009) analyzed the streamwise vorticity equation experimentally and numerically and showed that the turbulent stress distribution and the centrifugal forcing terms are important for the existence of the outer bank cell in curved open channel flow. Furthermore Blanckaert & de Vriend (2004) stated that accurately modeling the outer bank cell requires a

turbulence model which can transfer turbulent kinetic energy unto the mean flow. In line with the statement of Blanckaert & de Vriend (2004), Booij (2003) showed that a large-eddy simulation model is able to capture the outer bank cell correctly, whereas a RANS model with a linear k-ε closure is unable to do so. The outer bank cell is a more subtle feature of curved river bends, which requires advanced turbulence modeling to capture correctly.

The adaptation of meandering rivers occur at large temporal and spatial scales which mean a 3D modeling approach is unfeasible for natural river systems. Therefore, simplified 1D models are still widely used (e.g. Ikeda et al. 1981, Struiksma & Crosato 1989, Seminara & Tubino 1989, Odgaard 1989, Abad & Garcia 2006, Crosato 2008). In such models the river bend is characterized by the following important quantities: the average depth *H,* the average width *B*, the radius of curvature *R* and the bulk velocity *U* (cf. Figure 1). Furthermore the velocity is often modeled using a linear approximation as shown in Figure 1. The transverse distribution of the water depth is described in a similar way (cf. Blanckaert & de Vriend (2010) for a review of commonly used approximations of the streamwise velocity and water depth in 1D models). Inspite of all the progress in describing meandering rivers (e.g. 2D approaches (Mosselman 1992, Darby et al. 2002, Duan & Julien 2005, Chen & Duan 2008) and recently even a full 3D approach (Ruther & Olsen, 2007)), there is no model for meander evolution which includes enough detail to capture the complex outer bank dynamics accurately.

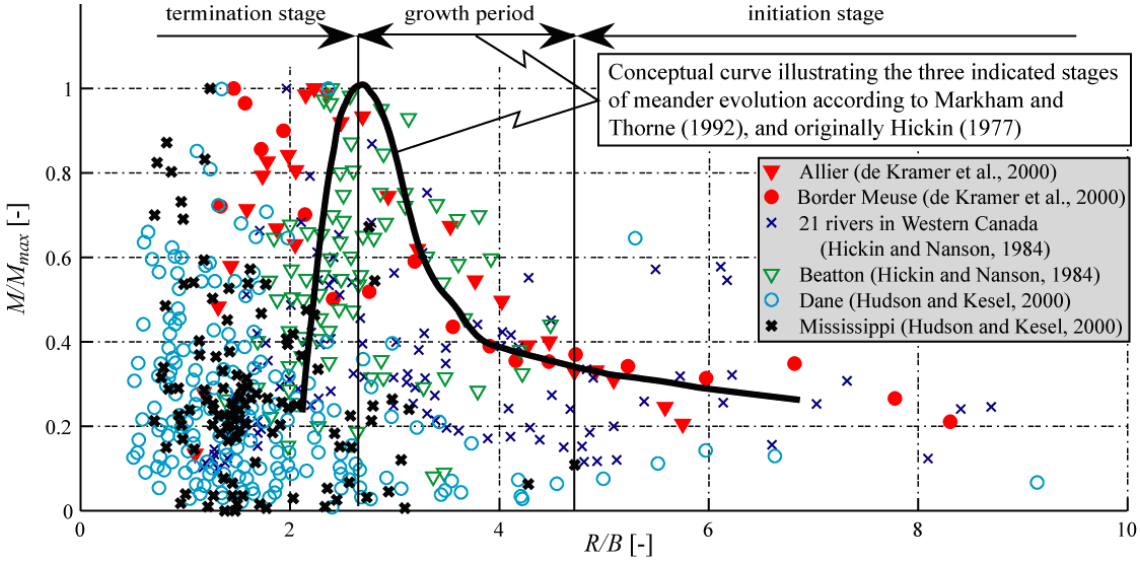

Figure 2 Modified conceptual curve after Hickin & Nanson (1984) illustrating the normalized rate of yearly migration M/M_{max} of meandering rivers as a function of *B/R* (modified from Blanckaert 2011)

Hickin and Nanson (1975, 1984) showed that the yearly migration rate, which is closely linked to the bank erosion rate, in meandering rivers depends on the ratio between the curvature radius *R* and the river width *B* (Their research was originally formulated in terms of *R/B*, but for ease of comparison we will discuss their result in terms of *B/R*). Hickin and Nanson (1984) show that for small increasing *B/R* the migration rate increases, subsequently reaches a maximum for a certain *B/R* (typically $B/R \approx 0.33$ to 0.5) and then the migration rate decreases again for large increasing *B/R* (see Figure 2).

Hickin and Nanson distinguish various phases in the migration rate in Figure 2 for *B/R* smaller than 0.23 the initiation stage, growth stage *B/R* between 0.23 and 0.38, termination stage *B/R* greater than 0.38. These values roughly correspond to the definitions of mildly, moderately and sharply curved bends. Plotting the migration rate as dependent on *B/R* shows great scatter, particularly in the sharply curved range denoted by $B/R > 0.5$ (R/B < 2). This indicates that there are hydrodynamic and morphodynamic processes which are not accounted for and are important for the migration rate.

Ikeda et al. (1981) postulated that the migration rate can be modeled as a migration coefficient multiplied by the velocity excess ΔU. Pizzuto and Mecklenburg (1989) provided some evidence in favour

of the formulation by Ikeda et al., yet this simple parameterization cannot account for the complex near bank hydrodynamics.

Blanckaert and de Vriend (2010) developed a nonlinear model for the velocity redistribution in open-channel bends. Blanckaert (2011) applied this model to investigate the velocity excess at the outer bank for the case of axi-symmetric flow (i.e. fully developed flow in an infinite length bend) and found that it is determined by the two control parameters B/R and $C_f^{-1}H/B$. The first control parameter expresses how sharply curved an individual bend is, whereas the second is characteristic of a river reach and accounts for the roughness and the shallowness.

The effect of the outer bank cell for varying depths and bank inclinations on the main flow was studied experimentally by Duarte (2008) and Blanckaert (2011). This paper will extend the experimental investigation into the complex outer bank hydrodynamics on the main flow by performing a parameter study based on the two control parameters B/R and $C_f^{-1}H/B$ using a large eddy simulation code with advanced turbulence modeling capabilities. The main objectives of this paper can be summarized as follows:

1. How does the outer bank shear stress depend on the width to radius ratio B/R and the inverse aspect ratio H/B?
2. What is the role of the near bank hydrodynamics on the bank shear stress?
3. Can the behavior found in the observations by Hickin and Nanson be explained by the complex near-bank hydrodynamics?
4. Can the results from the large eddy simulations be parameterized such that the modeling of bank shear stress can be improved in 1D meander models?

2 PARAMETER STUDY

Various straight and curved channel setups have been setup and run according to the control parameters $C_f^{-1}H/B$ and B/R. In this section the Large-eddy simulation model will briefly be discussed, subsequently the choice and setup of the simulation cases will be explained, and finally a short guide to the interpretation of the model results will be given.

2.1 *Large eddy simulation model description*

The present study uses the large-eddy simulation model originally developed by Eggels et al. (1994) and Pourquié (1994), and further developed by van Balen (2010) in his study on sharply curved bend flow. For this study the effect of the sub-grid scale eddies is modeled through the classical Smagorinsky model with a Smagorinsky constant $C_s = 0.1$.

To save computation time, a wall function approach is used at the solid boundaries. For smooth walls, the viscous sublayer, the buffer layer and the log layer are captured as follows:

$$\begin{aligned} u^+ &= y^+ && \text{for} \quad y^+ \le 5 \\ u^+ &= 5.0\ln(y^+) - 3.05 && \text{for} \quad 5 < y^+ < 30 \\ u^+ &= 2.5\ln(y^+) + 5.5 && \text{for} \quad y^+ \ge 30 \end{aligned} \tag{1}$$

The left hand side $u^+ = u/u_*$ is the dimensionless velocity and the dimensionless wall coordinate is given by $y^+ = y\,u_*/\nu$ where u_* is the friction velocity and ν is the kinematic viscosity. The distance to the wall is given by y. For rough boundaries the following wall function is used:

$$u^+ = 2.5\ln\left(y \cdot \frac{30}{k_s}\right) \qquad \text{for} \quad y > k_s/30 \tag{2}$$

where k_s is the Nikuradse roughness height typically expressed as a constant times the sediment diameter (see e.g. Kamphuis 1974, van Rijn 1984), Further details about the model and its numerical implementation may be found in van Balen (2010).

2.2 *Case descriptions*

For axi-symmetric flow, Blanckaert (2011) showed the relative importance of the scaling parameters $C_f^{-1}H/B$ and B/R for the distribution of the streamwise velocity in fully developed flow. Therefore we varied the simulation setups according to the control parameters listed in Table 1. The side walls were considered to be hydraulically smooth and the bottom boundary roughness was modeled using a Nikuradse roughness height of 6 millimeters. The range of the control parameters in Table 1 for $C_f^{-1}H/B$ is between 11.8 and 50. This range corresponds well to the range typically found in experimental setups. In natural river bends $C_f^{-1}H/B$ generally varies between 5 and 10 (Blanckaert 2011). The range of the parameter $C_f^{-1}H/B$ and the rectangular cross-sections in the axi-symmetric simulations mean that the chosen set of simulations is not representative of natural river bends. The simulations have been simplified such that the role of the near bank behavior on the bank shear stress can be identified clearly. Therefore this study is an initial investigation into role of the near bank hydrodynamics on the bank shear stress, and could provide clues to understanding the effect of the near bank hydrodynamics on the bank shear stress in naturally occurring rivers.

Various simulations have been setup and they may be identified by the case name. The first letter corresponds to the inverse aspect ratio H/B, ('A' stands for shallow depth H/B = 0.08, 'B' corresponds to the medium depth H/B = 0.12, and 'C' represents the deepest cases H/B = 0.16). At the second position, the increasing value of the digit corresponds to a decreasing width to radius of curvature ratio B/R which runs from a sharply curved channel (B/R = 0.77) to a straight channel (B/R = 0).

Table 1 Overview of simulation cases. H is the water depth, B is channel width, R is the radius of curvature at the centerline, U describes the bulk velocity, k_s is the Nikuradse roughness height at the bed. N_s, N_n, N_z denote the grid dimensions in streamwise, transverse and vertical direction, respectively. B/R denotes the width to radius of curvature ratio, H/B is the inverse aspect ratio and $C_f^{-1}H/B$ is a parameter accounting for roughness and the shallowness of the simulation

Case	H (m)	B (m)	R (m)	U (m/s)	k_s (mm)	N_s	N_n	N_z	B/R	H/B	$C_f^{-1}H/B$
A1	0.108	1.3	1.7	0.43	6	240	240	20	0.77	0.08	11.8
A2	0.108	1.3	2.7	0.43	6	240	240	20	0.48	0.08	13.1
A3	0.108	1.3	3.7	0.43	6	240	240	20	0.36	0.08	13.9
A4	0.108	1.3	6.2	0.43	6	240	240	20	0.21	0.08	15.1
A5	0.108	1.3	10	0.43	6	240	240	20	0.13	0.08	16.3
A6	0.108	1.3	18.6	0.43	6	240	240	20	0.07	0.08	17.6
A7	0.108	1.3	40	0.43	6	240	240	20	0.03	0.08	19.3
A8	0.108	1.3	100	0.43	6	240	240	20	0.01	0.08	20.7
A9	0.108	1.3	∞	0.43	6	240	240	20	0.00	0.08	20.7
B1	0.159	1.3	1.7	0.43	6	228	228	28	0.77	0.12	18.6
B2	0.159	1.3	2.7	0.43	6	228	228	28	0.48	0.12	20.4
B3	0.159	1.3	3.7	0.43	6	228	228	28	0.36	0.12	21.9
B4	0.159	1.3	6.2	0.43	6	228	228	28	0.21	0.12	24.3
B5	0.159	1.3	10	0.43	6	228	228	28	0.13	0.12	26.1
B6	0.159	1.3	18.6	0.43	6	228	228	28	0.07	0.12	28.3
B7	0.159	1.3	40	0.43	6	228	228	28	0.03	0.12	31.1
B8	0.159	1.3	100	0.43	6	228	228	28	0.01	0.12	35.6
B9	0.159	1.3	∞	0.43	6	228	228	28	0.00	0.12	36.7
C1	0.206	1.3	1.7	0.43	6	216	216	36	0.77	0.16	25.4
C2	0.206	1.3	2.7	0.43	6	216	216	36	0.48	0.16	28.1
C3	0.206	1.3	3.7	0.43	6	216	216	36	0.36	0.16	30.0
C4	0.206	1.3	6.2	0.43	6	216	216	36	0.21	0.16	33.4
C5	0.206	1.3	10	0.43	6	216	216	36	0.13	0.16	35.7
C6	0.206	1.3	18.6	0.43	6	216	216	36	0.07	0.16	39.6
C7	0.206	1.3	40	0.43	6	216	216	36	0.03	0.16	44.1
C8	0.206	1.3	100	0.43	6	216	216	36	0.01	0.16	48.8
C9	0.206	1.3	∞	0.43	6	216	216	36	0.00	0.16	53.1

2.3 *Method of analysis*

The large-eddy simulations produce a detailed set of flow quantities which can be seen from the grid resolution (cf. Table 1). Figure 3b,c) show the streamwise velocity as well as every fifth secondary flow vector in vertical and in transverse direction. The bank shear stress distribution along the solid boundaries of the domain is shown in Figure 3d) which enables us to determine the average outer bank shear stress. As present meander models are far less detailed we reduced the results from the large-eddy simulation into variables which are commonly used in a 1D meander model (Figure 3a)). The depth averaged streamwise velocity U_s, for instance, is approximated as:

$$U_S \approx U\left(1+\frac{\alpha_S}{R}n\right) \tag{3}$$

where the degree of freedom is given by α_s/R and can be interpreted as the normalized transverse gradient of the streamwise velocity. The degree of freedom α_s/R is determined from a least squares linear fit of the depth averaged streamwise velocity across the full cross section. The velocity excess can then be expressed as $\Delta U = 0.5\, BU\alpha_s/R$.

For straight channel flow, the general assumption is that the velocity is uniform in the cross-section and the bank shear stress is generally approximated as

$$\tau_{bank} \approx \rho C_{f,bank} U^2 \tag{4}$$

where ρ is the density of water, U is the bulk velocity and $C_{f,bank}$ is parametrization of the bank roughness.

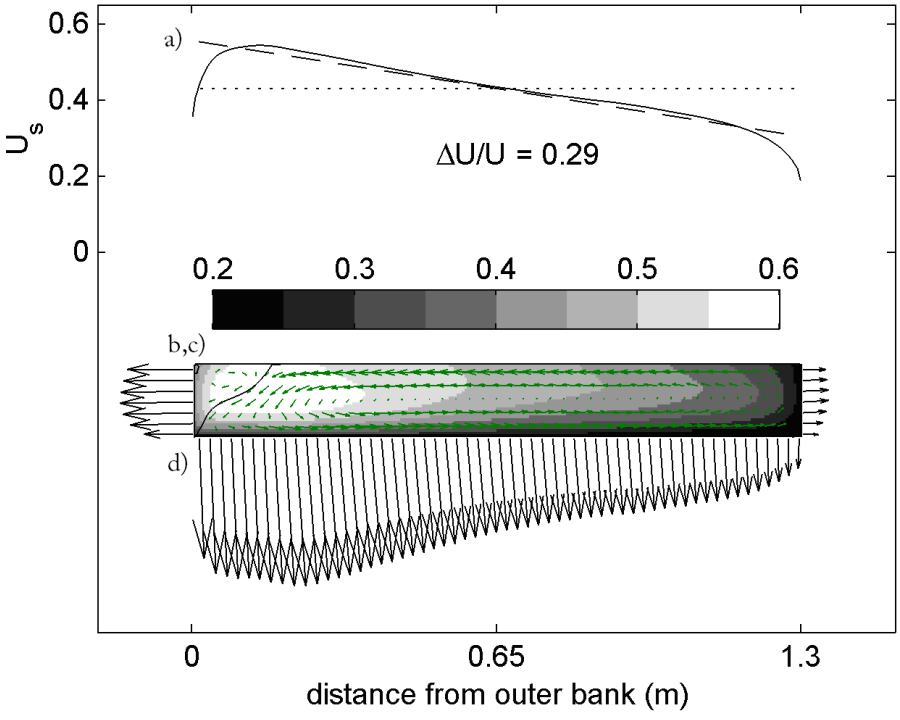

Figure 3 a) Illustration for case B7 with H = 0.159 m, R = 40 m showing a) the depth averaged velocity distribution (m/s) and first order approximation using a least squares fit over the full cross-section (cf. equation 3) b) streamwise velocities (m/s) given by shaded portion c) secondary flow vectors showing the centre region cell and the outer bank cell on inside of the rectangular cross-section d) shear stress distribution and orientation (outward normal to the rectangular cross-section is in streamwise direction). For sake of clarity only every fourth shear stress vector and the every fifth cross-circulation vector are plotted

In curved channel flow approximating the outer bank shear stress is no longer trivial as there extra complicating factors: firstly the flow is no longer uniform in the cross-section and secondly near the bank a complex near bank flow pattern exists. These two aforementioned factors will undoubtedly play a role

in the bank shear stress approximation. To account for the non-uniformity of the streamwise velocity we consider the near bank velocity rather than the bulk velocity in equation (4). In the context of a 1D model the near bank velocity may be approximated as the sum of the bulk velocity and the velocity excess ($U + \Delta U$). Due to the complexity of the near bank hydrodynamics and the simplicity of the formulation a correction factor may be required. Therefore we introduce a correction factor $\psi_{\text{outer bank}}$ which can be determined on the basis of the various simulations.

$$\tau_{bank} \approx \rho \psi_{outer\ bank} C_{f,bank} U_{bank}^2 \tag{5}$$

3 RESULTS

3.1 *Velocity excess*

For the simulations done we plotted the normalized velocity excess $\Delta U/U$ as a function of increasing bend sharpness B/R in Figure 4. For B/R equal to 0 (i.e. the straight channel limit) $\Delta U/U$ is equal to zero as well, which can be explained on the grounds of symmetry. For small and increasing values of B/R the strength of the centre region cell increases linearly and causes the outward transport of streamwise momentum which leads to an increase in $\Delta U/U$. The slope of the increase of $\Delta U/U$ for increasing B/R is higher for increasing H/B. This may be attributed to the centre-region flow strength which depends linearly on the water depth for small B/R. Another reason which may play a modest role for the higher slope of $\Delta U/U$ is the reduced influence of the constant Nikuradse roughness height for increasing depth, thereby allowing the core of the streamwise momentum to be closer to the outer bank.

The normalized velocity excess subsequently obtains a maximum for a certain B/R. For increasing aspect ratio H/B the velocity excess occurs for lower values of B/R and its value is higher.

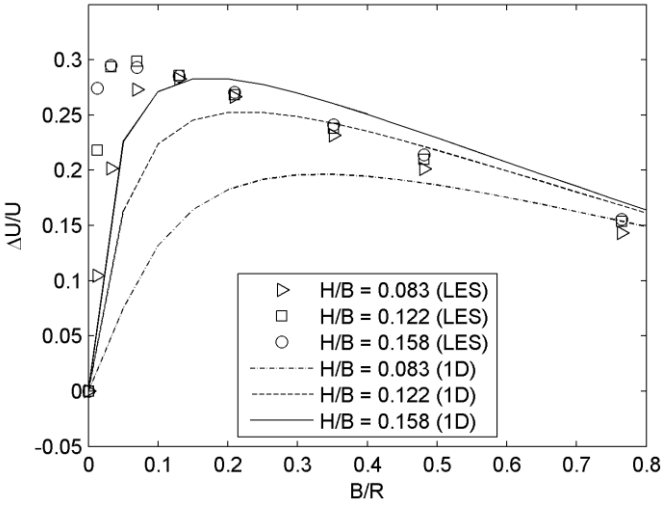

Figure 4 Normalized velocity excess $\Delta U/U$ as function of the parameter B/R

For large increasing values of B/R the value of $\Delta U/U$ decreases. For large B/R the primary and secondary flow interact strongly with each another. Consequently, the streamwise velocity profile is no longer logarithmic but becomes constant near the free surface and exhibits a maximum at around $z = H/3$. The secondary flow (at the centerline $n = 0$) is thereby weakened as it basically depends on the vertical gradient in the streamwise velocity and shows hardly any increase for increasing B/R. This phenomenon has been explained as the saturation of secondary flow (Blanckaert 2009). Due to the increase in the flow velocities near the bed, and increased turbulence production, an increase of friction is felt by the flow which causes the secondary flow strength to reduce even further. Owing to the saturation and subsequent reduction of the secondary flow, the exchange of primary and secondary flow reduces thereby reducing outward transport of momentum. This explains why the normalized velocity excess decreases for increasing B/R. The results of the normalized velocity excess for axi-symmetric bend flow are consistent

with the parameter study by Blanckaert (2011) who used a 1D model without curvature restrictions (Blanckaert & de Vriend 2010) (cf. Figure 4).

3.2 *Bank shear stress*

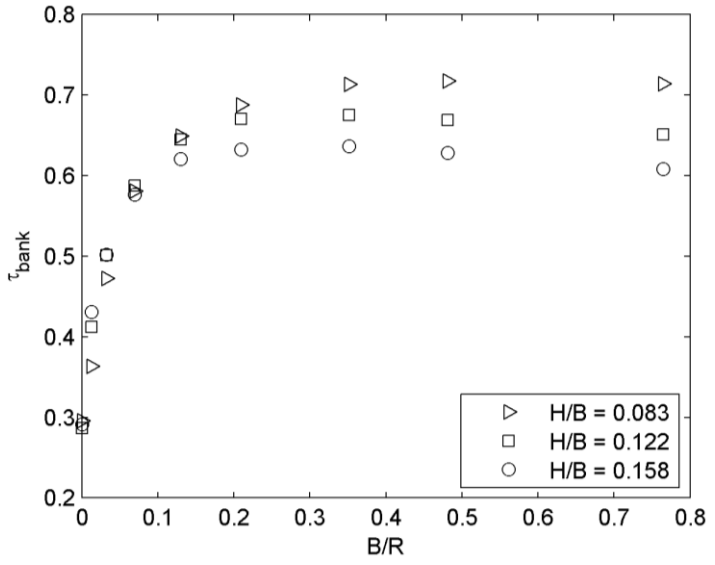

Figure 5 Depth averaged shear stress at the outer bank τ_{bank} as function of the parameter *B/R* and the ratio *H/B*

As a next step we plotted the average shear stress on the outer bank against the parameter *B/R* in Figure 5. The outer bank shear stress τ_{bank} increases for small increasing *B/R*. This can be explained by the increase of the velocity excess $\Delta U/U$ which results in higher velocities near the bank. For large increasing *B/R*, τ_{bank} no longer increases obtaining a maximum value and subsequently even decreases very slightly. The velocity excess shown in Figure 4 shows a clear decrease for large increasing B/R and so this cannot explain why the behavior of the bank shear stress τ_{bank}.

The effect of increasing *H/B* for large *B/R* results in a decrease of the bank shear stress. Figure 4 shows that the velocity excess does not play a big role is this regard as the velocity excess shows almost equal values for increasing *H/B* at large *B/R*.

The apparently different behaviour in the distribution of the velocity excess compared to the bank shear stress implies that a correction coefficient $\psi_{outer\ bank}$ is required to relate the outer bank shear stress with the velocity excess.

The relation to behavior found by Hickin and Nanson (Figure 2) is not immediately apparent, but it is clear that for sharply curved the outer bank shear stress becomes more or less constant. Van Balen (2010) showed that the width averaged bed shear stress increases for increasing *B/R*. As erosion formulations are closely linked to the bank shear stress (e.g. Mosselman, 2005), this suggests that sharp channel bends will have a preference for deepening instead of migrating laterally.

3.3 *Bank shear stress parameterization*

Present 1D models cannot account for the complex near bank processes and are therefore unable to correctly predict bank shear stresses. As explained in section 2.3 we will derive a correction factor $\psi_{\text{outer bank}}$ which will account for the complex near-bank hydrodynamics. Using equation (4) we solved for the unknown $C_{f,bank}$ using the bank shear stress obtained from the straight channel cases (A9, B9 and C9) and subsequently using the curved flow cases (A1-A8, B1-B8 and C1-C8) the correction factor $\psi_{outer\ bank}$ was derived. This factor represents the increase in friction due to the complex near-bank hydrodynamics. Figure 6 shows the values for the correction factor. It may be seen that $\psi_{outer\ bank}$ increases monotonically for increasing *B/R* and decreasing *H/B*.

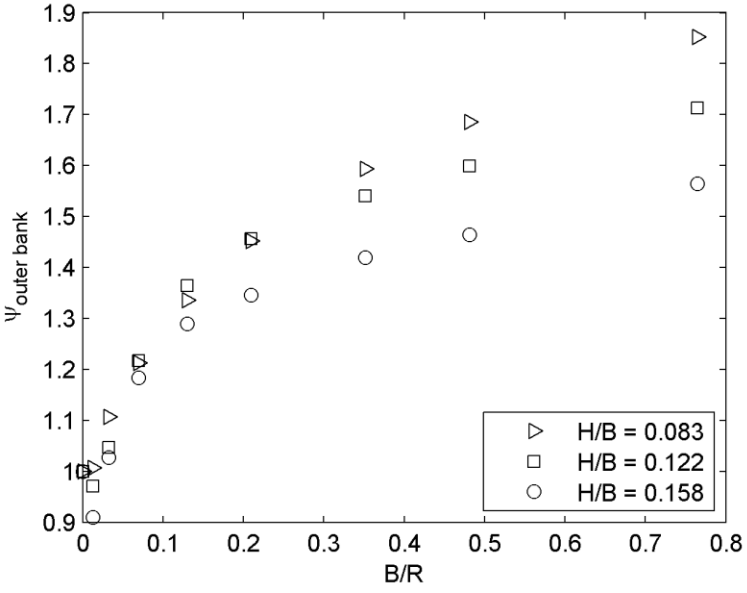

Figure 6 The relative dependence of the increase of friction $\psi_{outer\ bank}$ depending on the parameter *B/R* and the inverse aspect ratio *H/B*

4 CONCLUSIONS

By means of a parameter study by means a of large-eddy simulations the outer bank shear stresses were studied. Based on the study the following conclusions can be drawn:

Firstly, the outer bank shear stress depends on both the width to radius of curvature ratio *B/R* and the inverse aspect ratio *H/B*. For small increasing *B/R* the bank shear stress increases strongly. For large increasing *B/R* the growth of the bank shear stress stagnates and even slightly decreases. For increasing values of *H/B* for *B/R*>0.1, the bank shear stress decreases in magnitude.

Secondly, a comparison with linear approximation of the streamwise velocity showed that the complex near bank hydrodynamics result in a larger bank shear stress than would be expected from the square of the near bank velocity multiplied with a bank friction factor.

Thirdly, based on the simulations and findings by van Balen (2010) it was observed that for increasing *B/R* the bank shear stresses decrease slightly, whereas the bed shear stresses increase. These preliminary findings suggest that sharp channels tend to deepen instead of migrate laterally.

Finally, a parameterization was developed which allows the parameterization of bank shear stresses in axi-symmetric flows based on a bank friction coefficient $C_{f,bank}$, the bulk velocity U, the velocity excess ΔU and a correction coefficient $\psi_{outer\ bank}$ which depends on the ratios *H/B* and *B/R*.

5 ACKNOWLEDGEMENTS

The Dutch Technology Foundation (STW), applied science division of NWO is gratefully acknowledged for the research grant DCB.7780. The support of Deltares is also gratefully acknowledged. The second author was partially funded by the Chinese Academy of Sciences fellowship for young international scientists under Grant No. 2009YA1-2 and by the Sino-Swiss science and technology cooperation for joint research, project GJH20908. Gratitude is extended to Wim van Balen for kindly providing the large-eddy simulation model and useful discussions.

6 REFERENCES

Abad JD, Garcia MH. 2006. RVR Meander: a toolbox for re-meandering of channelized streams. Computers and Geosciences 32: 92–101.

Bathurst JC. Thorne CR, Hey RD. 1977. Direct measurements of secondary currents in river bends. Nature 269, 504–506.

Blanckaert K. 2009. Saturation of curvature‐induced secondary flow, energy losses, and turbulence in sharp open-channel bends: Laboratory experiments, analysis, and modeling, J. Geophys. Res., 114, F03015, doi:10.1029/2008JF001137.

Blanckaert K. 2011. Hydrodynamic processes in sharp meander bends and their morphological implications, J. Geophys. Res., 116, F01003, doi:10.1029/2010JF001806.

Blanckaert K, de Vriend HJ. 2003. Nonlinear modeling of mean flow redistribution in curved open channels, Water Resour. Res., 39(12), 1375, doi:10.1029/2003WR002068.

Blanckaert K, de Vriend HJ. 2004. Secondary flow in sharp open‐channel bends, J. Fluid Mech., 498, 353‐380, doi:10.1017/S0022112003006979.

Blanckaert K, de Vriend HJ. 2010. Meander dynamics: A nonlinear model without curvature restrictions for flow in open‐channel bends, J. Geophys. Res., 115, F04011, doi:10.1029/2009JF001301.

Blanckaert K, Graf WH. 2004. Momentum transport in sharp open‐channel bends, J. Hydraul. Eng., 130(3), 186‐198, doi:10.1061/(ASCE)0733-9429(2004)130:3(186).

Booij R. (2003), Measurements and large eddy simulations of the flows in some curved flumes, J. Turbul., 4(8), doi:10.1088/1468-5248/4/1/008.

Boussinesq, J. (1868). M´emoire sur l'influence de frottement dans les mouvements r´eguliers des fluides; xii - essai sur le mouvement permanent d'un liquide dans un canal horizontal axe circulaire. J. Math. Pures Appl., 13(2).

Chen D, Duan JG. 2008. Case Study: Two-Dimensional Model Simulation of Channel Migration Processes in West Jordan River, Utah. J. Hydaul. Eng. 134 pp.315-327. doi:10.1061/(ASCE)0733-9429(2008)134:3(315)

Crosato A. 2008. Analysis and modelling of river meandering, Ph.D. dissertation, Delft Univ. of Technol., Delft, Netherlands.

Darby SE, Alabyan AM, van de Wiel MJ. 2002. Numerical simulation of bank erosion and channel migration in meandering rivers, Water Resour. Res., 38(9), 1163, doi:10.1029/2001WR000602.

de Kramer J, Wilbers A., van den Berg J, Kleinhans M. 2000. De Allier als morfologisch voorbeeld voor de Grensmaas. Deel II:Oevererosie en meandermigratie (in Dutch), Natuurhist. Maandbl., 89, 189–198.

Duan JG, Julien P. 2005. Numerical simulation of the inception of meandering channel. Earth Surf. Processes Landforms, 30, 1093–1110.

Duarte A. 2008, An experimental study on main flow, secondary flow and turbulence in open‐channel bends with emphasis on their interaction with the outer‐bank geometry, Ph.D. thesis 4227, EPFL, Lausanne, Switzerland.

Eggels, JGM, Unger F, Weiss MH, Westerweel J, Adrian RJ, Friedrich R, and Nieuwstadt FTM. 1994. Fully developed turbulent pipe flow: a comparison between direct numerical simulation and experiment. J. Fluid Mech. 268, 175–209.

Hickin EJ. 1977. Hydraulic factors controlling channel migration, in Research in Fluvial Geomorphology: Proceedings of the 5th Guelph Geomorphology Symposium, edited by R. E. Davidson‐Arnott and W. Nickling, pp. 59–66, Geobooks, Norwich, U.K.

Hickin EJ, Nanson GC. 1975. The character of channel migration on the Beatton River, northeast British Columbia, Canada. Bulletin of the Geological Society of America 86 487–94.

Hickin EJ, Nanson GC. 1984. Lateral migration rates of river bends. Journal of Hydraulic Engineering 110(11): 1557–1567. doi:10.1061/(ASCE)0733-9429(1984)110:11(1557).

Hudson PF., Kesel RH. 2000. Channel migration and meander-bend curvature in the lower Mississippi River prior to major human modification, Geology, 28(6), 531–534.

Ikeda S, Parker G, Sawai K. 1981. Bend theory of river meanders. Part 1. Linear development, J. Fluid Mech., 112, 363–377, doi:10.1017/S0022112081000451.

Kalkwijk JPT, de Vriend, HJ. 1980. Computation of the flow in shallow river bends, J. Hydraul. Res., 18(4), 327–342.

Kamphuis JW. 1974. Determination of sand roughness for fixed beds. J. Hydraul. Res., 12(2).

Markham AJ, Thorne CR. 1992, Geomorphology of gravel‐bed river bends, in Dynamics of Gravel‐Bed Rivers, edited by P. Billi et al., pp. 433–456, Wiley, Chichester, U.K.

Mosselman E. 1992. Mathematical modelling of morphological processes in rivers with erodible cohesive banks. PhD dissertation, Communications on Hydraulic and Geotechnical Engineering, No.92-3, Delft University of Technology, ISSN 0169-6548.

Mosselman E. 2005. Basic equations for sediment transport in cfd for fluvial morphodynamics. Chapter 4, Computational Fluid Dynamics,Applications in Environmental Hydraulics. Bates PD, Lane SN, Ferguson RI (Eds), John Wiley and Sons, Ltd.: United Kingdom, 71–89.

Odgaard AJ. 1989. River‐meander model. I: Development, J. Hydraul. Eng., 115(11), 1433–1450, doi:10.1061/(ASCE)0733-9429(1989)115:11(1433).

Olesen KW. (1987), Bed topography in shallow river bends, Ph.D. dissertation, Delft Univ. of Technol., Delft, Netherlands.

Pizzuto J, Meckelnburg T. 1989. Evaluation of a linear bank erosion equation, Water Resour. Res., 25, 1005–1013, doi:10.1029/WR025i005p01005.

Pourquie MJBM. 1994. Large-eddy simulation of a turbulent jet. Ph.D. thesis, Delft University of Technology, Delft.
Ruther N, Olsen NRB. 2007. Modelling free-forming meander evolution in a laboratory channel using three-dimensional computational fluid dynamics. Geomorphology, 89(3-4):308–319. doi:10.1016/j.geomorph.2006.12.009.
Seminara G, Tubino M. 1989. Alternate bar and meandering: free, forced and mixed interactions. In: River Meandering, Water Resources Monograph, AGU, Vol. 12, eds. Ikeda S. & Parker G., pp. 267-320, ISBN 0-87590-316-9.
Struiksma N, Crosato A. 1989. Analysis of a 2D bed topography model for Rivers. In: River Meandering, Water Resources Monograph, AGU, Vol. 12, eds. Ikeda S. & Parker G., pp. 153-180. ISBN 0-87590-316-9.
Thomson, J. 1876. On the origin of windings of rivers in alluvial plains, with remarks on the flow of water round bends in pipes. Proc. R. Soc. London, 25:5–8.
van Balen, W. 2010. Curved open-channel flows: a numerical study, Ph.D. dissertation, Delft Univ. of Technol., Delft, Netherlands.
van Balen, W., Uijttewaal WSJ, and Blanckaert K. 2009. Large-eddy simulation of a mildly curved open-channel flow. J. Fluid Mech. vol. 630, pp. 413–442. doi:10.1017/S0022112009007277.
van Bendegom, L. (1947), Eenige beschouwingen over riviermorphologie en rivierverbetering (in Dutch), De Ingenieur, 59(4), 1–11.
van Rijn L. 1984. Sediment transport, part I: Bed load transport. J. Hydraul. Eng. 110(10) 1431-1456.